Nanoscale Control and Manipulation of Molecular Transport in Chemical Analysis

Paul W. Bohn

Department of Chemical and Biomolecular Engineering, Department of Chemistry and Biochemistry, University of Notre Dame, Notre Dame, Indiana 46556; email: pbohn@nd.edu

Annu. Rev. Anal. Chem. 2009. 2:279–96

First published online as a Review in Advance on February 26, 2009

The *Annual Review of Analytical Chemistry* is online at anchem.annualreviews.org

This article's doi: 10.1146/annurev-anchem-060908-155130

1936-1327/09/0719-0279$20.00

Key Words

nanochannels, nanopores, stochastic sensing, stimulus-responsive materials, nanoelectrodes

Abstract

The ability to understand and control molecular transport is critical to numerous chemical measurement strategies, especially as they apply to mass-limited samples in nanometer-scale structures. The characteristics of nanoscale structures and devices highlighted in the examples discussed in this article include enhanced mass transport, accessing novel physical behavior, large surface-to-volume ratio, diminished background signals, and the fact that molecular characteristics can dominate the behavior of the structure. The control of nanoscale transport is physically embodied in different structures and experiments. Those structures and experiments highlighted here are featured because of their centrality (nanochannels and nanopores), their connection to more familiar macroscale phenomena (nanoelectrodes), and/or their ability to introduce control (stimulus-responsive materials) or because they represent especially interesting possibilities (stochastic sensing structures).

1. INTRODUCTION

The ability to understand and control molecular transport is critical to numerous chemical measurement strategies. In the past, understanding of transport processes has targeted length scales at which continuum descriptions of fluid flow are adequate. However, recent advances have focused on materials and structures designed at the molecular level and constructed with control of composition and structure on molecular and supermolecular length scales. Chemical analysis stands to benefit greatly from molecular-level control of transport and from architectures capable of manipulating the physical placement of species in space and time with nanometer-level precision—the subjects of this article.

Molecular transport mediated by structures of nanometer (1 nm $< d <$ 100 nm) characteristic dimensions is a critical component of many separation technologies (1, 2) and sensor paradigms (3–6). Independent of the type of force field—e.g., voltage, pressure—used to drive transport, the unique characteristics of nanoscale structures ensure transport characteristics fundamentally different from those in larger micrometer- and millimeter-scale structures. These differences are only beginning to be understood, yet it is clear that understanding and control of transport on the nanoscale will enable the construction of novel devices that can address refractory problems in molecular separations and chemical analysis. Thus, it is critical to establish intelligent control over molecular transport in space and time at small length scales. Intelligent control implies materials and structures that can sense molecular characteristics, e.g., size, charge, and molecular shape, and then generate signals that control transport on the basis of those characteristics. Specifically, researchers aspire to manipulate (separate, isolate, react, and detect) low-mass samples with the same precision and level of control currently possible with bench-scale samples. Thus, it is worthwhile to state clearly the driving forces behind chemical analysis strategies involving nanometer-scale structures:

1. Mass transport is significantly enhanced relative to large structures. It is more rapid, owing to the $t \sim \langle x^2 \rangle / D$ dependence, and can display a different dimensionality, as in hemispherical diffusion to a point-like reactive site on a surface.
2. New physical phenomena come into play when the size of the structure becomes commensurate with physical scaling lengths, e.g., transport in nanocapillaries of a size comparable to the Debye length in ionic solution.
3. Small structures exhibit enhanced surface-to-volume ratios, so surface phenomena are naturally accentuated.
4. Small volumes generate smaller background signals, as exemplified by the decreased background fluorescence in single-molecule fluorescence experiments.
5. Regenerating probe species after a measurement is facilitated, if the mass loading is small, easing the logistics of making successive measurements.
6. Sufficiently small structures are dominated by molecular properties, e.g., single-molecule conduction experiments implemented such that the limiting element is a molecule arrayed between source and drain nanoelectrodes.

Despite these compelling factors, making chemical measurements at ultrasmall structures presents several significant challenges:

1. Small structures interact with a small total number of molecules. Therefore, signals that scale with molecular population are diminished relative to measurements in larger structures. Depending on the readout, small structures can be exceptionally susceptible to environmental noise.
2. Fabrication of small-scale structures can be tedious and expensive, especially to the extent that they involve expensive lithographies.

3. Interfacing to small structures must be carefully addressed because there is a mismatch between the scales (e.g., volumes, lengths, times for transport, and equilibration) characterizing the nanostructure and the leads that connect it to the external world.
4. The ergodic hypothesis, which undergirds much of macroscale sampling theory, needs to be explicitly justified for small structures, meaning that statistical fluctuations in chemical properties—reflecting, for example, fluctuations in the chemical potential—can play a much more important role than in larger structures and samples.

These opportunities and challenges form the essential motivation for experiments using control of nanoscale transport for applications in chemical analysis. The control of nanoscale transport is physically embodied in many different types of structures and experiments, a few of which are highlighted here because of their centrality (nanochannels and nanopores), their connection to more familiar macroscale phenomena (nanoelectrodes), their ability to introduce control in a natural way [stimulus-responsive materials (SRMs)], or because they represent especially interesting future possibilities (stochastic sensing structures). Owing to space limitations of this review, a number of related areas, e.g., laser tweezers, are not discussed, even though they are widely applicable and represent interesting topics.

2. NANOCHANNELS AND NANOPORES

Although the engineering drivers for reducing the size of laboratory devices are clear (e.g., reduced materials costs, reduced power consumption, less waste, and lower operating costs), the case for doing science at reduced dimensions needs to be made more carefully. Factors that justify the added experimental complexity of working at the nanometer scale include (*a*) access to new transport phenomena, (*b*) exploitation of the enhanced surface-to-volume ratio, (*c*) use of diffusion as a viable transport mechanism, and (*d*) integration of large molecules or molecular complexes into small (1–10-nm) physical structures. Nanochannel/nanopore systems that address all four criteria can be constructed.

All studies of electrokinetic transport in nanometer-scale cylindrical capillaries trace their origin to a seminal 1965 paper by Rice & Whitehead (7), which described, within the Debye-Hückel approximation, the behavior of electroosmosis, streaming potential, current-density distributions, and the electroviscous effect in cylindrical capillaries of nanometer dimensions. If one begins with the Poisson-Boltzmann equation for a narrow cylindrical capillary at small ζ potential,

$$\frac{1}{r}\frac{d}{dr}\left(r\frac{d\varphi}{dr}\right) = \kappa^2\varphi, \tag{1}$$

where

$$\kappa = \sqrt{8\pi ne^2/\varepsilon kT} \tag{2}$$

is the inverse Debye length, it yields a solution,

$$\varphi = \varphi_0\frac{I_0(\kappa r)}{I_0(\kappa a)}, \tag{3}$$

where I_0 is the modified Bessel function of the first kind. Equation 3 allows the charge density to be recovered directly by use of the Poisson equation. For an infinite cylindrical tube, the equation of motion under a combination of electrical and pressure-driven flow can then be written

$$\frac{1}{r}\frac{d}{dr}\left(r\frac{dv_z}{dr}\right) = \frac{1}{\eta}\frac{dp}{dz} - \frac{F_z}{\eta}, \tag{4}$$

where the body force, F_z, is driven by the action of the applied field on the net charge density in the double layer, $\rho(r)$. The important result from this analysis is the establishment of two flow regimes. When $\kappa a \gg 1$, the radial velocity profile, $v_z(r)$, reduces to the classical result, i.e., the plug flow familiar from studies of capillary electrophoresis in micrometer-scale capillaries is recovered. When $\kappa a \sim 1$, $v_z(r)$ is proportional to $(a^2 - r^2)$, behavior that is equivalent to Poiseuille flow at nanometer dimensions. Ramsey and coworkers (8) used an elegant one-dimensional confinement channel system to test and verify experimentally predictions of the radial velocity profile. Another notable early effort to describe flow in small-scale structures was the investigation of potential-driven flow in slit-pore geometries by Levine and coworkers (9). They were the first to explore the ratio of channel and bulk viscosities at various values of the zeta potential, ζ, and κa in a model that allowed for double-layer overlap and arbitrary ζ, showing an electroviscous retardation effect in nanochannels.

The transport problem in nanopores is typically determined by three related scaling lengths: the Debye length, κ^{-1}; the pore diameter, a; and the molecular size of the principal species being transported, which can be specified by a molecular diameter, b, or by an effective size, such as the radius of gyration, R_G. Much recent work has sought to clarify the relative importance of these scaling lengths. The most direct and easily measured nanoscale characteristic is the conductivity, σ, which is linearly related to the ion concentration, $\sigma \approx \mu_+ n_+ + \mu_- n_-$, where $\mu_{+/-}$ and $n_{+/-}$ are the ion mobilities and concentrations, respectively. Employing an elegant slit-pore geometry in Si, Schoch and coworkers (10, 11) demonstrated that, at low ionic strength, σ becomes independent of n in nanopores. This behavior is attributed to the surface charge density, $\Gamma_{+/-}$, which requires a certain population of solution counterions to achieve charge neutrality within the nanopore, thereby pinning the conductivity at a value higher than that for the bulk. Dekker and colleagues (12) used a similar slit-pore geometry to measure the streaming conductance, Σ_P, as a function of $n_{+/-}$ and found that they had to relate ζ to the surface charge density developed by deprotonation of the Si-OH surface moieties to model the behavior with salt concentration correctly. Recently a significant effort to model these systems has also examined, in particular, the role of the κa product in determining the behavior of fluid transport in nanoscale tubes and slits (13–15). Notable in this regard is the work of Qiao & Aluru (14), who studied the scaling of electrokinetic transport in a sub-5-nm slit-pore geometry by comparing the results of molecular dynamics calculations with results from continuum theory and found a significant departure from continuum behavior. These researchers found that the interfacial viscosity of water in contact with the pore wall increases dramatically with increasing $\Gamma_{+/-}$, resulting in a nearly immobile population of counterions at the wall of the nanopore. Furthermore, they found, consistent with the experimental work of Schoch et al. (10, 11), that the conductivity is dominated by the surface charge density.

Efforts to fabricate structures that can probe these relationships have focused principally on slit pores and single nanopores in membranes. A number of research groups have developed robust strategies for the fabrication of planar slit pores connecting in-plane microfluidic channels, exploiting the fact that only a single dimension of the nanoslit need be of nanometer dimensions (16). Ramsey and coworkers (17) were the first to realize that the integration of in-plane nanoporous structures with microfluidic channels could be used to concentrate an analytical sample by exploitation of the vast transport differences between structures at the micrometer and nanometer scales. This result was extended by Zhang & Timperman (18), who used nanocapillary array membranes (NCAMs), and by Han and colleagues (19), who used slit pores in Si to achieve 10^7-fold enhancement in the concentrations of labeled proteins and peptides. Studies of individual nanopores have followed up on the seminal work by Crooks and coworkers, who used carbon nanotubes as templates for the fabrication of single-pore membranes (20), to examine the behavior of single nanopores fabricated either by the templated growth of conformal coatings (21) or by

the preparation of single asymmetric (conical) nanopores in polymer membranes (22–24). Interest in such structures follows directly from the ability to realize active electronic functions such as rectification (25) and field-effect-transistor (26) and bipolar-transistor (27) action with ionic currents, work that is the successor to the pioneering contributions by Martin and coworkers (28) in the use of charge to control ionic transconductance across NCAMs. Finally, in a distinct approach to the problem, Orwar and coworkers (29–31) have developed a system of surface-immobilized unilamellar vesicles connected by small (50–150-nm-radius) nanotubes that can support the same types of pressure-driven and electrokinetic flows realized in more conventional structures as well as unusual attributes, such as Marangoni flow caused by viscous coupling of the nanotube fluid to surface tension gradient–driven wall motion.

The numerous ways in which nanoscale features interact differentially with molecules on the basis of size, shape, and charge have raised hopes that nanopores could be exploited to achieve extraordinarily fast and efficient separations. By fabricating one surface of a rectangular microfluidic channel from a porous alumina membrane, Sano and coworkers (32) achieved a type of size exclusion separation without requiring direct transmission through the nanopores. If flow past a nanopore-containing surface is considered, smaller molecules spend more time exploring the pores in the nanoporous membrane than do their larger counterparts, and the net progress of the smaller molecules down the channel is impeded relative to the larger molecular components. Although the observed separation efficiency was not high, proof-of-principle was demonstrated, and this geometry has the advantage of not requiring the prohibitive pressure heads associated with packed microfluidic channels. López and coworkers (33) have studied the separation behavior of the slit-pore geometry in planar format. They found that by changing the width of the slit at constant ionic strength, i.e., by varying κa, they could reverse the order of elution in an electrophoretic separation of small-molecule dyes. By far the most heavily studied system for separation in nanoscale structures is DNA (34–36) because of its centrality in molecular and systems biology, because of its intrinsically interesting entropic trapping behavior (37), and because, as a self-avoiding structure, it allows fundamental questions in the statistical mechanics of polymers to be posed and answered (35). Finally, the capacity to use nanopores and NCAMs as affinity chromatography substrates has been studied, most notably by Bruening and coworkers (38, 39), who are exploiting the high surface-to-volume ratio of these materials to prepare high-capacity preconcentration substrates to sequester phosphopeptides and phosphorylated proteins. Such proteins could subsequently be characterized by matrix-assisted laser desorption ionization (MALDI) mass spectrometry (viz. **Figure 1**). Efforts like this, to control transport and achieve interesting separations, are critically dependent on the capacity to control the environment inside the nanopore, a problem that has received both theoretical (40) and experimental (41) attention. Recently, the Martin (42) and Stroeve (43) groups developed schemes for controlling the charge state and the chemical environment inside nanopores. Yang, Majumdar, and colleagues (44) performed an elegant series of sequential modifications to the interior of a nanopore in order to deconvolute the effects of charge and pore occlusion. Majumdar and coworkers (26) further utilized the field-effect-transistor concept to achieve active control of the motion of charged proteins through nanochannels. Active transport control has also been achieved by coupling stimuli-responsive polymers and coatings to the interior or the entrance/exit of nanopores to realize transport control by environmental perturbations (45–47; see below).

Applications that exploit the inherent capacity of nanopores/channels for differential transport to achieve molecular separations build upon a large body of prior work focused on the hindered transport of species in narrow channels. Stevens and colleagues (48, 49) used the method of reflections to account for membrane pore wall interactions with solutes at low ζ and found little effect at $\kappa a > 1$, although the researchers encountered difficulties with protein agglomeration under

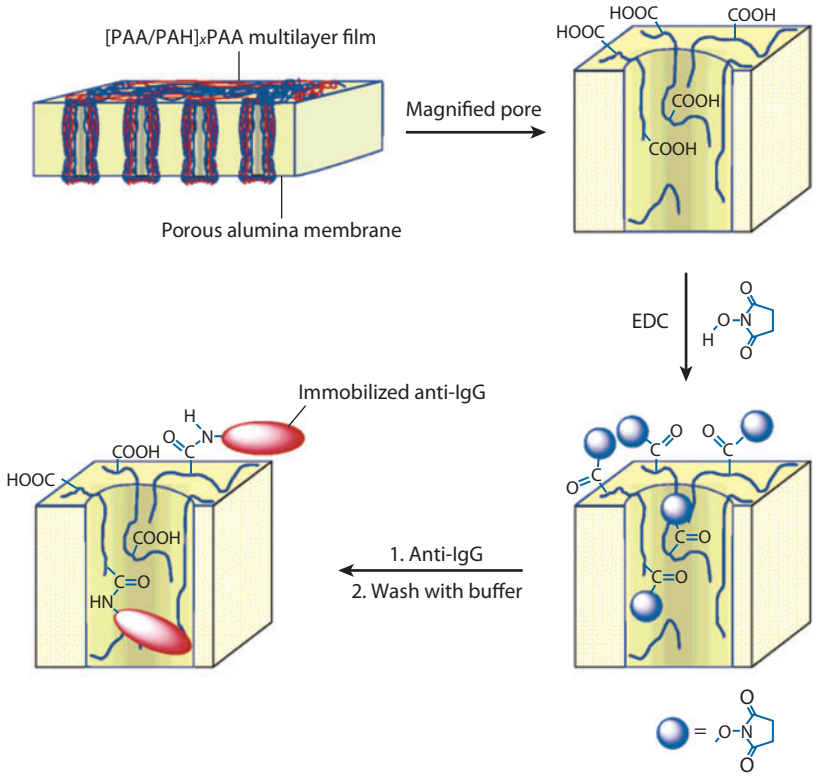

Figure 1

Scheme for derivatizing the nanopores of an alumina nanocapillary array membrane with high-efficiency antibody-based capture elements. In the strategy of Bruening et al. (38), the surface carboxylic acid groups of poly(acrylic acid) (PAA) are activated with *N*-(3-dimethylaminopropyl)-*N′*-ethylcarbodiimide (EDC) and *N*-hydroxysuccinimide. This enables the covalent attachment of antibodies, whereas succinimidyl esters that do not react with protein can subsequently be hydrolyzed to reconstitute the acidic groups. Reproduced with permission from Reference 38. Copyright 2006, American Chemical Society.

some conditions. Although Chun and colleagues (50) considered diffusive transport, their work is important in considering the partitioning and conformational behavior of model polyelectrolytes in nanometer-diameter pores. They used a Green function theory with an effective step length renormalized by monomer-monomer interactions and divided the transport into the elementary steps of partitioning (between bulk and pore) and transport (within the pore), which are determined by the relative sizes of a, κ^{-1}, and R_G. Chun et al. (50) found partitioning to be determined by the interplay between steric and electrostatic factors; at the small κ limit the electrostatic potential within the pore determines the partitioning behavior at all values of a and R_G.

In addition to the direct use of nanochannels to effect molecular separations and analyses, Sweedler, Bohn, and their coworkers (51–56) have exploited NCAMs to control the spatial and temporal position of molecules in three-dimensional microfluidic architectures, thereby realizing integrated microfluidic circuitry, as illustrated in **Figure 2**. Kuo et al. (51, 52) carried out experiments in devices composed of a poly(vinylpyrrolidone) (PVP)-coated polycarbonate nuclear track etched (PCTE) membrane embedded between two vertically separated poly(dimethylsiloxane) (PDMS) microchannels. In the system of Kuo et al., PDMS exhibits a negative surface charge and PVP a positive surface charge at pH 8. Such conditions cause the preferred electroosmotic

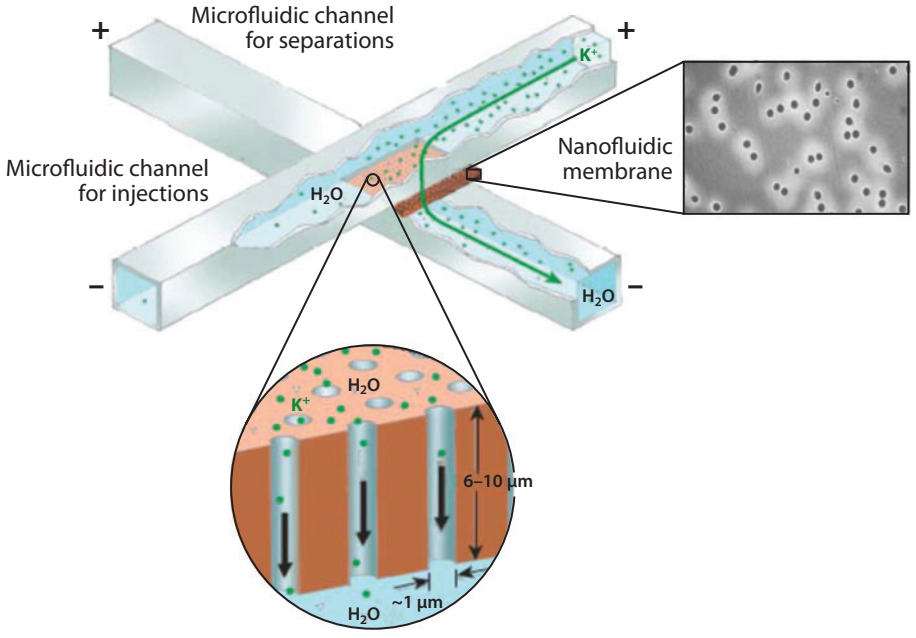

Figure 2

An illustration of the integrated microfluidic concept. A nanocapillary array membrane (NCAM) fluidically couples two vertically separated orthogonal microfluidic channels. The NCAM presents several new possibilities for molecular manipulation during transport in micro-/nanoscale systems. The figure shows a scanning electron microscopy image of the NCAM and a schematic illustration of the fluidic coupling. Copyright 2008, Institute of Electrical and Electronic Engineers.

flow vectors for the microchannels and nanochannels to be in opposite directions. In their trans-NCAM electrokinetic transport experiments, the net-transport direction is determined by NCAM pore-size. The properties of the hybrid microfluidic/nanofluidic systems described above enable a variety of unit analytical operations such as gated injections (53), fraction collection (54), sample-stream mixing (55), and analyte preconcentration (17–19) to be carried out in a single, integrated device. Specifically, the trinary nature of fluid flow (reverse, off, and forward) across integrated nanofluidic elements allows for the externally controllable transport of fluidic bands throughout three-dimensional networks. The forward and reverse states have clear applications in gated injections and fraction collection. The off state is equally important in that it enables chemically distinct environments to be maintained within an interconnected device (56).

3. STIMULUS-RESPONSIVE MATERIALS

For several decades there has been strong interest in manipulating the macroscopic properties of membranes and vesicles through external perturbations. Materials that respond to perturbations in their surroundings by changing their physical state, i.e., SRMs, constitute dynamically responsive systems that can be used to manipulate molecular transport, especially in combination with nanoscale anisotropic structures, such as nanopores. Environmental responsiveness has been engineered into materials that respond to external stimuli, including pH (57–59), temperature (60, 61), ionic strength (62), irradiation (63), the presence of specific molecules (analytes) (64), and applied voltage (65, 66). Typically, the active agent contains a functional group that responds to

the perturbation: lipophilic alkyl chains in the case of temperature, an azobenzene moiety capable of undergoing *cis-trans* isomerization in the case of light, ferrocene or viologen in the case of redox-active agents, or a Brønsted basic site in the case of pH.

SRMs are frequently fabricated in polymeric forms to realize the combined benefits of stimulus-responsive behavior with the robustness of a macromolecular construct. Researchers often exploit properties of polymers or oligomers in solution by preparing the corresponding surface adlayer or by grafting the polymer directly to the surface of interest. For example, hydrogels constitute one principal class of SRMs. pH responsiveness is achieved by the inclusion of acidic (e.g., acrylic acid) or basic (e.g., allylamine) monomers, either alone or in combination with an aprotic acrylate such as hydroxyethylmethacrylate (HEMA). Temperature responsiveness is most often achieved with materials such as poly(*N*-isopropylacrylamide) (PNIPAm), which display a structural transition at a specific temperature. For example, PNIPAm undergoes a conformational change from a disordered random coil to a globular state at its lower critical solution temperature (LCST). This phenomenon is shared by poly(alkylene oxides) and elastin-like polypeptides (67). PNIPAm is particularly interesting in that its LCST occurs in the physiological range, near 32°C. The chief interest in electric-field-responsive SRMs is in the behavior of monoliths composed of one or more hydrogels, typically for applications as electric-field-actuated mechanical components, in artificial muscle, for example (68).

Both physical and chemical methods have been exploited to separate molecules using membranes on the basis of their charge (28, 69), chemical interaction (69), and size (70). Of course, membranes have been used extensively in size-selective separations, for example, in dialysis and ultrafiltration, but in these applications the membrane is designed for a specific molecular-size threshold. Grafting membrane surfaces with polymers with tunable properties is an effective route to obtain environmentally sensitive composite membranes. Physical changes in the grafted film can be triggered by the same stimuli responsible for manipulating larger-scale films, namely pH (71), ionic strength, solvent quality (72), electric field, light, redox potential, and temperature, resulting in stimuli-responsive film-grafted membranes with high mechanical strength, quick response to external signals, the ability to transport both neutral and charged molecules, and strong resistance to degradation due to covalent bonding between substrate and polymer.

Of particular interest are temperature-induced volume changes in polymers grafted in and around nanopore openings to alter the effective pore diameter. Contraction and dilation of polymer films can be based on reversible ionization of the functional groups, solvent intrusion and extrusion into the polymer network, and phase separation. Most investigations have centered on temperature-induced transitions owing to their importance in physiological systems. Both positive temperature-sensitive polymers, which shrink when cooled below their upper critical solution temperature (UCST), and negative temperature-sensitive polymers, which contract when heated above their LCST, have been identified. Temperature-sensitive gels that exhibit LCST phase transition can be prepared from *N*-substituted acrylamide derivatives, e.g., PNIPAm, *N*,*N*′-diethylacrylamide, *N*-acryloylpyrrolidine, *N*-vinylisobutyramide, and *N*-acryloylpiperidine (73, 74).

Thermodynamic properties of PNIPAm, which as discussed above undergoes a dramatic volume transition in water at its LCST near 32°C, were first reported in References 75 and 76. Hirokawa & Tanaka (77) reported discontinuous phase transition properties, and López and coworkers (78) described how the degree of polymerization and surface coverage of PNIPAm brushes tethered onto planar surfaces affect temperature-manipulated volume transitions. This distinctive behavior of PNIPAm has been attributed to its rapid alteration in hydrophilicity (79). At temperatures lower than the LCST, PNIPAm expands owing to hydrogen bond formation between hydrophilic segments in the side chains of the polymer and water. The hydrogen bonds

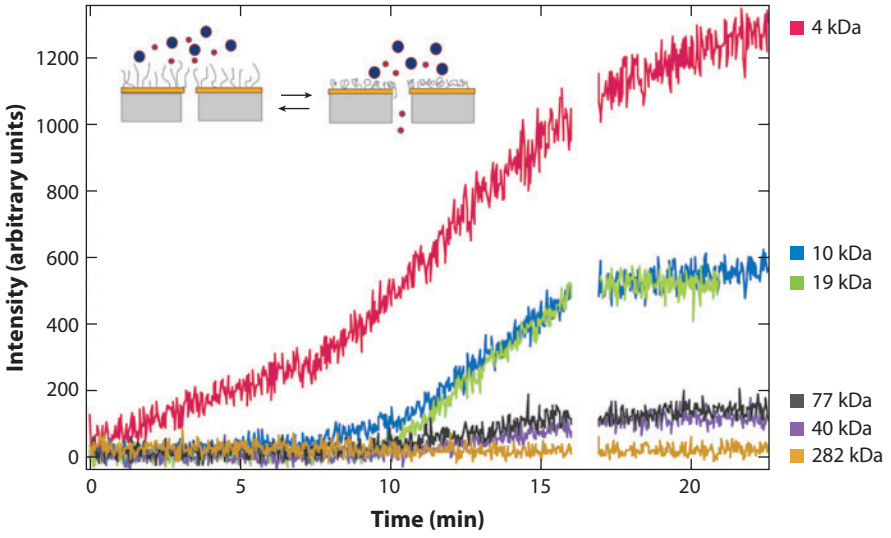

Figure 3

Thermal gating of a poly(*N*-isopropylacrylamide) (PNIPAm)-coated nanocapillary array membrane (NCAM) to dextrans of various molecular weights. Temperature program: 0–7 min, 25°C; 7–16 min, 40°C; 16–17 min, replacement of the feed solution; and 17–23 min, 25°C. (*Inset*) Schematic of the application of a thermally gated transition to effect a size-selective capture of the smaller component of a binary mixture. Reproduced with permission from Reference 45. Copyright 2007, American Chemical Society.

form a stable hydration shell around the hydrophobic groups, which leads to large water uptake at low temperatures. Above the LCST, the polymer-solvent interactions are disrupted, hydrogen bonding is weakened, and polymer-polymer hydrophobic interactions dominate, causing an abrupt collapse in polymer free volume owing to the release of entrapped water. In exploitation of these dramatic volume changes, for example, to construct size-selective NCAMs (e.g., **Figure 3**), the response time is critical. In contrast to conventional network structures, which have relatively rigid chain ends, these terminally grafted polymer brushes exhibit rapid conformational changes (80); the speed is attributed to the mobility of free chain ends (81). The temperature sensitivity of PNIPAm has also been exploited to achieve actively controlled thermoresponsive, size-selective transport switching by grafting PNIPAm brushes onto a Au-coated NCAM through the use of atom transfer radical polymerization (ATRP) (45).

4. NANOELECTRODES

Nanoelectrodes, ultramicroelectrodes in the earlier literature, inherently exploit the interplay between electron transfer rates and mass transport on the nanoscale. As highlighted in a recent review by Arrigan (82), the principal advantage conferred by studying electron transport at nanoelectrodes derives from the enhanced mass transport accruing to the hemispherical diffusion profile at a small electrode, compared with the semi-infinite planar diffusion to a planar or macroscale electrode. Much research has examined the construction of nanoelectrodes and nanoelectrode assemblies, and although a number of ingenious strategies have been devised, there are three principal routes to fabrication: (*a*) the use of a templating medium, like a nuclear track-etched membrane or a processed block copolymer, to direct the electrochemical deposition of a small-radius electrode (83); (*b*) etching of dielectric-encased wires to expose a small metallic area (viz. **Figure 4**) (84);

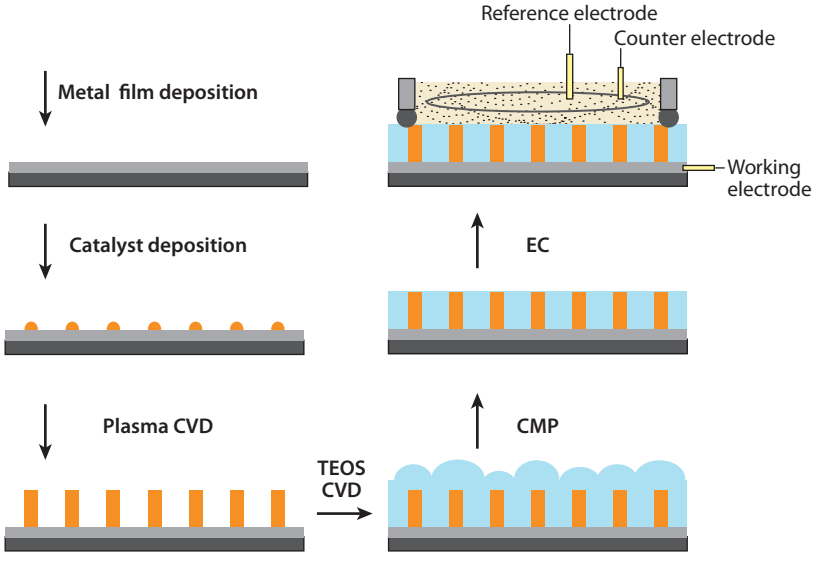

Figure 4

Schematic illustration of the formation of carbon nanotube electrode arrays. Metal deposition is uniform over the substrate film; catalyst is deposited in a defined pattern; plasma chemical vapor deposition (CVD) is used to grow carbon nanotubes from catalyst initiators; CVD of tetraorthosilicate (TEOS) produces a SiO_2 film; the SiO_2-carbon nanotube composite is planarized by chemomechanical polishing (CMP); and electrochemistry (EC) is performed in a standard three-electrode potentiostatically controlled cell with reference, counter, and working electrodes. Reproduced with permission from Reference 82. Copyright 2004, Royal Society of Chemistry.

and (*c*) deposition of a narrow wire encased in dielectric layers, followed by cleavage of the sample perpendicular to the wire to expose its cross section as a nanoband electrode (85).

Fabrication capabilities have progressed to the point that it is now possible to construct electrodes with radii of a few atoms. Lemay and coworkers (86) developed electrode structures by drilling small apertures in back-thinned silicon nitride membranes by focused ion beam (FIB) milling followed by slow evaporation of Au to yield pyramidal Au structures down to 2 nm. In addition, there has been recent interest in the construction of electrodes separated by small gaps (87). The electrodes are typically nanoelectrodes, and the nature of their placement confers special properties on the mass transfer from which electrochemical currents are ultimately derived. White & White (88) have modeled the behavior of a single electroactive molecule in an electrochemical cell composed of two spherical shell electrodes separated by a 1–20-nm gap. Whereas both theoretical and experimental studies of redox processes at nanoelectrodes indicate sigmoidal *i-E* characteristics, White & White's model found that long-range electron transfer produces nonsigmoidal-shaped *i-E* characteristics when the interelectrode separation becomes comparable to the characteristic redox tunneling decay length—another example of the interesting phenomena that arise when physical scaling lengths coincide with device dimensions. Nanochannels can be nanoelectrodes too, as demonstrated by Macpherson and coworkers (89), who studied the iontophoretic transport of $Fe(CN)_6^{4-}$ across track-etched poly(ethylene terphthalate).

In addition to the transfer of electrons, altered conduction in nanowires and nanogaps derivatized with single molecules spanning the gap has been an increasingly popular subject of study. Studies of chemically mediated electrical conduction in ultrasmall junctions can all ultimately be traced to the defining vision of pioneers like Aviram & Ratner (90) for molecular electronics. From

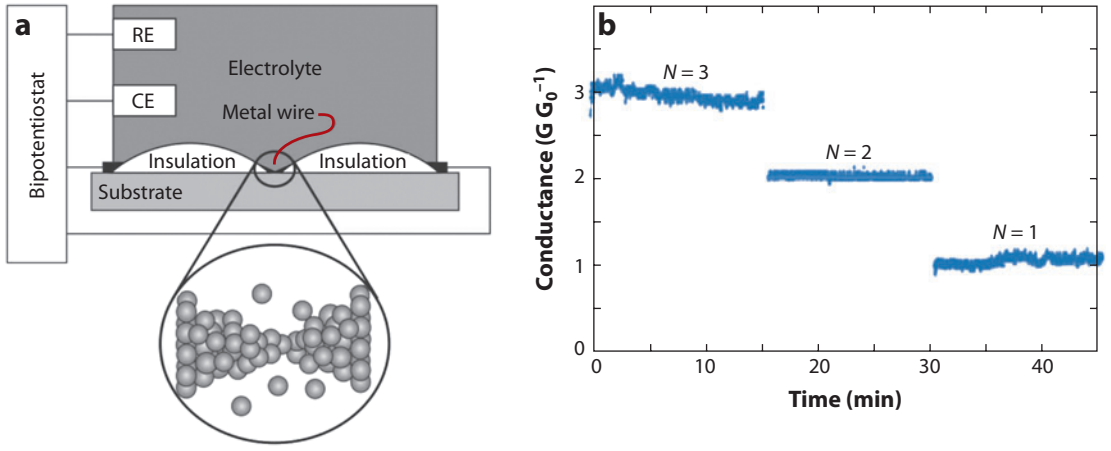

Figure 5

(*a*) Schematic illustration of the electrochemical method used by Tao and coworkers to fabricate atomscale metallic junctions. A metal wire, covered with an insulator except in the region where the junction is to be formed, is exposed to electrochemical etching. (*b*) Atomscale junctions prepared from Cu exhibit quantized conductance at $G = 1$, 2, and 3 G_0. Reproduced with permission from Reference 108. Copyright 2005, American Chemical Society.

the measurement of electrical conduction of metal oxide thin films for the detection of gas-phase contaminants in hostile environments (91), to the use of organic (92) or inorganic (93) semiconducting nanowires, in which sensing occurs by altering the width of the space charge region (94, 95), applications of conduction measurements in chemical sensing span an enormous range.

More recently it has become possible to realize conducting junctions constructed of small arrays of atoms or even single molecules. Junctions composed entirely of metal atoms have been studied extensively since the mid-1990s (96, 97), and their conduction properties are interpreted within the Landauer formulation, which interprets electron transport in the ballistic regime as transmission between two perfect, but energetically offset, reservoirs (98). Some studies have addressed molecular adsorption at these junctions (99, 100), but most attention has focused on the preparation of molecule-sized gaps and the subsequent study of single-molecule conductance (101–103), the subject of recent comprehensive reviews (e.g., 104).

Of particular relevance to the control of transport on the nanoscale are studies in which small, i.e., atom-scale, gaps (105–107) or wires (108) are fabricated electrochemically. For example, Tao (108) introduced self-limiting electrochemical processes in the preparation of atomic-scale structures (viz. **Figure 5**). In their approach, directional electrodeposition was initiated between two electrodes separated by micrometer distances with a series impedance used to set a voltage threshold. When the local overpotential drops below the $E°$ value, deposition ceases in a self-limiting process. This work achieved reproducible nanowires characterized by constrictions only a few atoms wide. Such atom-scale junctions exhibit quantized conductance, measured in units of the conductance quantum, $G_0 = 2e^2/h = (12.9\ \text{k}\Omega)^{-1}$, a characteristic feature of structures in which conduction electrons are confined to the order of the Fermi wavelength, λ_F (~0.52 nm for Au at 300 K). In addition, an extensive body of work focused on utilizing electrochemically fabricated nanowires for sensing was developed by Penner and coworkers, who deposited nanowires of Pt, Pd, and other metals at atomic step edges on highly oriented pyrolytic graphite (109) by laterally defined electrodeposition (110). Pt and Pd nanowires were extraordinarily sensitive to the presence of H_2 (111), which was due to the modulation of rate-limiting electron transfer

across grain boundaries by H_2-induced lattice distortions. Ag-based nanowires were particularly effective sensor elements owing to the development of chemically responsive interfacial boundaries (112), which consist of semiconducting AgO/Ag_2O boundary layers that connect metallic Ag nanowire sections. These developments are particularly exciting because they move the molecular determination from the realm of bulk properties to structures dominated by quantum effects—in the case of the metallic nanowires the ballistic, rather than diffusive, propagation of electrons through the constriction.

5. STOCHASTIC SENSING

We end this brief survey by examining efforts to exploit the specific transport properties of biomimetic membranes supporting single copies of membrane-bound transport proteins. Reasoning that nature has evolved a variety of proteins to mediate the transport of specific ions, researchers have sought to integrate both natural and genetically engineered versions of these transport molecules with artificial membranes to realize constructs with special and controllable transport characteristics.

Technologically these efforts trace their genesis to the pioneering efforts to generate highly impermeable membrane structures (the so-called GΩ seal) for model electrophysiological and neurochemical studies. Although these structures continue to be invaluable for model studies of neurotransmission, their direct relevance to general schemes for chemical analysis is limited. The neurotransmission experiments do, however, point to platforms on which more general transport schemes can be constructed. The archetypes of these later efforts are the experiments by Bayley and coworkers (113) to exploit the special properties of the staphylococcal protein α-hemolysin. The experimental paradigm incorporates the protein, as a seven-member self-assembled pore structure, in an otherwise impermeable membrane and measures the ionic current induced by a DC bias potential applied across the membrane. The flux of ions, i.e., the current, is tightly coupled to the internal structure of the ion channel constituted in the middle of the barrel structure. Various schemes are then employed to modulate the ion flux through an external side chain that can, in the presence of specific chemical species, fold over and occlude the ion channel. Because single-molecule binding-unbinding events modulate the reconfiguration of the occluding appendage, the current passed takes on characteristics of a telegraph signal—hence the term stochastic sensing (114).

The great power and flexibility of the stochastic sensing platform derive from the ability to genetically engineer the properties of the side chain that projects into the lumen. For example, side chains specific for divalent cations have been prepared through histidine substitution (115), and side chains specific for the transport of a number of interesting analytes ranging from DNA (116) to second messengers such as IP3 (117) have been constructed.

Despite the great success of the generic approach, a number of concerns, such as the ultimate stability of single-protein sensors and the design flexibility offered by the α-hemolysin system, have spurred research into alternative pore-forming systems. Martin's group (118, 119) has studied the use of synthetic structures based on asymmetric conical nanopores for resistive pulse detection of analyte passage, and White and coworkers (120) have developed glass nanopore membranes for ion channel recording. Bayley and coworkers (121) have extended the approach to systems offering greater design flexibility, such as the monomeric β-barrel protein OmpG, which is derived from the membrane of *Escherichia coli*. Exploiting detailed molecular dynamics in combination with genetic engineering, Bayley and coworkers designed a variant of the OmpG proteins in which the background gating behavior is switched off, producing a low-background, "quiet" porin-based biosensor (e.g., **Figure 6**) (121). Finally, novel applications are beginning to occur on the basis

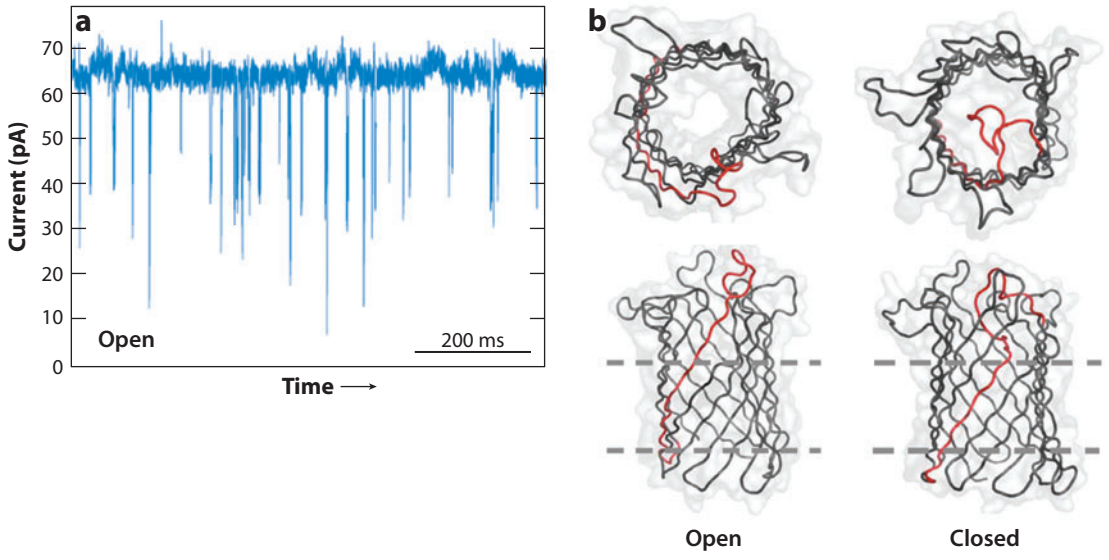

Figure 6

Schematic illustration of the use of a monomeric β-barrel based on OmpG for stochastic sensing. (*a*) Typical stochastic modulation of the transmembrane current by pore blockage. (*b*) Plan and cross-sectional renderings of the barrel structure in both open and closed configurations. The analyte-binding side chain is shown in red. Reproduced with permission from Reference 121. Copyright 2008, National Academy of Sciences.

of improved data collection and robust statistical treatments of the stochastic transport events. Kasianowicz and coworkers (122) introduced a single-molecule liquid-phase mass spectrometer to characterize poly(ethylene glycol) based on mass-dependent conductance states that result directly from mass-dependent residence times experienced by PEG oligomers translocating an α-hemolysin pore. Both the fabrication of new synthetic pore structures as well as the development of more robust molecular architectures promise to enhance the utility of these fascinating structures even further.

DISCLOSURE STATEMENT

The author is not aware of any affiliations, memberships, funding, or financial holdings that might be perceived as affecting the objectivity of this review.

ACKNOWLEDGMENTS

Work described here that was carried out in the author's laboratory was funded through grants from the Department of Energy (DE FG02 07ER15851), National Science Foundation (CHE 0807816 and CTS 0120978), and the Strategic Environmental Research and Development Program.

LITERATURE CITED

1. Koros WJ, Chern RT. 1987. Separation of gaseous mixtures using polymer membranes. In *Handbook of Separation Process Technology*, ed. RW Rousseau, pp. 862–964. New York: Wiley
2. Mitchell DT, Lee SB, Trofin L, Li N, Nevanen TK, et al. 2002. Smart nanotubes for bioseparations and biocatalysis. *J. Am. Chem. Soc.* 124:11864–65

3. Bein T, Brown K. 1989. Molecular sieve sensors for selective detection at the nanogram level. *J. Am. Chem. Soc.* 111:7640–41
4. Brolo AG, Gordon R, Leathem B, Kavanagh KL. 2004. Surface plasmon sensor based on the enhanced light transmission through arrays of nanoholes in gold films. *Langmuir* 20:4813–815
5. Haes AJ, Van Duyne RP. 2002. A nanoscale optical biosensor: sensitivity and selectivity of an approach based on the localized surface plasmon resonance spectroscopy of triangular silver nanoparticles. *J. Am. Chem. Soc.* 124:10596–604
6. Patolsky F, Zheng GF, Lieber CM. 2006. Nanowire-based biosensors. *Anal. Chem.* 78:4260–69
7. Rice CL, Whitehead R. 1965. Electrokinetic flow in a narrow cylindrical capillary. *J. Phys. Chem.* 69:4017–24
8. Ramsey JM, Alarie JP, Jacobson SC, Peterson NJ. 2002. Molecular transport through nanometer confined channels. In *Micro Total Analysis Systems 2002*, ed. Y Baba, S Shoji, AVD Bert, pp. 314–16. Dordrecht, Neth.: Kluwer Acad.
9. Levine S, Marriott JR, Robinson K. 1975. Theory of electrokinetic flow in a narrow parallel-plate channel. *J. Chem. Soc.* 71:1–11
10. Schoch RB, Renaud P. 2005. Ion transport through nanoslits dominated by the effective surface charge. *Appl. Phys. Lett.* 86:253111
11. Schoch RB, van Lintel H, Renaud P. 2005. Effect of the surface charge on ion transport through nanoslits. *Phys. Fluids* 17:100604
12. Van Der Heyden FHJ, Stein D, Dekker C. 2005. Streaming currents in a single nanofluidic channel. *Phys. Rev. Lett.* 95:116104
13. Conlisk AT, McFerran J, Zheng Z, Hansford D. 2002. Mass transfer and flow in electrically charged micro- and nanochannels. *Anal. Chem.* 74:2139–50
14. Qiao R, Aluru NR. 2005. Scaling of electrokinetic transport in nanometer channels. *Langmuir* 21:8972–77
15. Tessier F, Slater GW. 2006. Effective Debye length in closed nanoscopic systems: a competition between two length scales. *Electrophoresis* 27:686–93
16. Hug TS, de Rooij NF, Staufer U. 2006. Fabrication and electroosmotic flow measurements in micro- and nanofluidic channels. *Microfluidics Nanofluidics* 2:117–24
17. Khandurina J, Jacobson SC, Waters LC, Foote RS, Ramsey JM. 1999. Microfabricated porous membrane structure for sample concentration and electrophoretic analysis. *Anal. Chem.* 71:1815–19
18. Zhang Y, Timperman AT. 2003. Integration of nanocapillary arrays into microfluidic devices for use as analyte concentrators. *Analyst* 128:537–42
19. Wang YC, Stevens AL, Han JY. 2005. Million-fold preconcentration of proteins and peptides by nanofluidic filter. *Anal. Chem.* 77:4293–99
20. Sun L, Crooks RM. 1999. Fabrication and characterization of single pores for modeling mass transport across porous membranes. *Langmuir* 15:738–41
21. Goldberger J, Fan R, Yang PD. 2006. Inorganic nanotubes: a novel platform for nanofluidics. *Acc. Chem. Res.* 39:239–48
22. Harrell CC, Siwy ZS, Martin CR. 2006. Conical nanopore membranes: controlling the nanopore shape. *Small* 2:194–98
23. Mercik S, Siwy Z, Spohr R, Weron K. 2001. Characterization of the asymmetric action of a single pore in a track-etched membrane. *Acta Phys. Pol. B* 32:1605–19
24. Schiedt B, Healy K, Morrison AP, Neumann R, Siwy Z. 2005. Transport of ions and biomolecules through single asymmetric nanopores in polymer films. *Nucl. Instrum. Methods Phys. Res. B* 236:109–16
25. Cervera J, Schiedt B, Neumann R, Mafe S, Ramirez P. 2006. Ionic conduction, rectification, and selectivity in single conical nanopores. *J. Chem. Phys.* 124:104706
26. Karnik R, Castelino K, Majumdar A. 2006. Field-effect control of protein transport in a nanofluidic transistor circuit. *Appl. Phys. Lett.* 88:123114
27. Daiguji H, Yang PD, Majumdar A. 2004. Ion transport in nanofluidic channels. *Nano Lett.* 4:137–42
28. Nishizawa M, Menon VP, Martin CR. 1995. Metal nanotubule membranes with electrochemically switchable ion transport selectivity. *Science* 268:700–2

29. Dommersnes PG, Orwar O, Brochard-Wyart F, Joanny JF. 2005. Marangoni transport in lipid nanotubes. *Europhys. Lett.* 70:271–77
30. Karlsson A, Karlsson M, Karlsson R, Sott K, Lundqvist A, et al. 2003. Nanofluidic networks based on surfactant membrane technology. *Anal. Chem.* 75:2529–37
31. Karlsson M, Davidson M, Karlsson R, Karlsson A, Bergenholtz J, et al. 2004. Biomimetic nanoscale reactors and networks. *Annu. Rev. Phys. Chem.* 55:613–49
32. Sano T, Iguchi N, Iida K, Sakamoto T, Baba M, Kawaura H. 2003. Size-exclusion chromatography using self-organized nanopores in anodic porous alumina. *Appl. Phys. Lett.* 83:4438–40
33. Garcia AL, Ista LK, Petsev DN, O'Brien MJ, Bisong P, et al. 2005. Electrokinetic molecular separation in nanoscale fluidic channels. *Lab Chip* 5:1271–76
34. Gasparac R, Mitchell DT, Martin CR. 2004. Electrokinetic DNA transport in a nanopore membrane. *Electrochim. Acta* 49:847–50
35. Tegenfeldt JO, Prinz C, Cao H, Chou S, Reisner WW, et al. 2004. The dynamics of genomic-length DNA molecules in 100-nm channels. *Proc. Natl. Acad. Sci. USA* 101:10979–83
36. Tegenfeldt JO, Prinz C, Cao H, Huang RL, Austin RH, et al. 2004. Micro- and nanofluidics for DNA analysis. *Anal. Bioanal. Chem.* 378:1678–92
37. Han JY, Craighead HG. 2002. Characterization and optimization of an entropic trap for DNA separation. *Anal. Chem.* 74:394–401
38. Dai JH, Baker GL, Bruening ML. 2006. Use of porous membranes modified with polyelectrolyte multilayers as substrates for protein arrays with low nonspecific adsorption. *Anal. Chem.* 78:135–40
39. Dunn JD, Watson JT, Bruening ML. 2006. Detection of phosphopeptides using Fe(III)-nitrilotriacetate complexes immobilized on a MALDI plate. *Anal. Chem.* 78:1574–80
40. Adiga SP, Brenner DW. 2005. Flow control through polymer-grafted smart nanofluidic channels: molecular dynamics simulations. *Nano Lett.* 5:2509–14
41. Chen HY, Elkasabi Y, Lahann J. 2006. Surface modification of confined microgeometries via vapor-deposited polymer coatings. *J. Am. Chem. Soc.* 128:374–80
42. Hou SF, Wang JH, Martin CR. 2005. Template-synthesized protein nanotubes. *Nano Lett.* 5:231–34
43. Chun KY, Mafe S, Ramirez P, Stroeve P. 2006. Protein transport through gold-coated, charged nanopores: effects of applied voltage. *Chem. Phys. Lett.* 418:561–64
44. Karnik R, Castelino K, Fan R, Yang P, Majumdar A. 2005. Effects of biological reactions and modifications on conductance of nanofluidic channels. *Nano Lett.* 5:1638–42
45. Lokuge I, Wang X, Bohn PW. 2007. Temperature controlled flow switching in nanocapillary array membranes mediated by poly(*N*-isopropylacrylamide) polymer brushes grafted by atom transfer radical polymerization. *Langmuir* 23:305–11
46. Ito Y, Park YS, Yukio I. 2000. Nanometer-sized channel gating by a self-assembled polypeptide brush. *Langmuir* 16:5376–81
47. Schwarz B, Schonhoff M. 2002. Surface potential driven swelling of polyelectrolyte multilayers. *Langmuir* 18:2964–66
48. Ennis J, Zhang H, Stevens G, Perera J, Scales P, Carnie S. 1996. Mobility of protein through a porous membrane. *J. Membr. Sci.* 119:47–58
49. Ho AK, Perera JM, Dunstan DE, Stevens DR. 1999. Measurement and theoretical modeling of protein mobility through membranes. *AlChE J.* 45:1434–50
50. Park PJ, Chun M-S, Kim J-J. 2000. Partitioning and conformational behavior of polyelectrolytes confined in a cylindrical pore. *Macromolecules* 33:8850–57
51. Kuo TC, Cannon DM Jr, Chen YN, Tulock JJ, Shannon MA, et al. 2003. Gateable nanofluidic interconnects for multilayered microfluidic separation systems. *Anal. Chem.* 75:1861–67
52. Kuo TC, Cannon DM Jr, Shannon MA, Bohn PW, Sweedler JV. 2003. Hybrid three-dimensional nanofluidic/microfluidic devices using molecular gates. *Sens. Actuators A* 102:223–33
53. Cannon DM Jr, Kuo T-C, Bohn PW, Sweedler JV. 2003. Nanocapillary arrays produce gated analyte injection for separations and analysis in three-dimensional microfluidic architectures. *Anal. Chem.* 75:2224–30
54. Tulock JJ, Shannon MA, Bohn PW, Sweedler JV. 2004. Microfluidic separation and gateable fraction collection for mass-limited samples. *Anal. Chem.* 76:6419–25

55. Kuo T-C, Kim H-K, Cannon DM Jr, Shannon MA, Sweedler JV, Bohn PW. 2004. Nanocapillary array membranes effect rapid mixing and reaction. *Angew. Chem. Int. Ed.* 43:1862–65
56. Fa K, Tulock JJ, Sweedler JV, Bohn PW. 2005. Profiling pH gradients across nanocapillary array membranes connecting microfluidic channels. *J. Am. Chem. Soc.* 127:13928–33
57. Hester JF, Olugebefola SC, Mayes AM. 2002. Preparation of pH-responsive polymer membranes by self-organization. *J. Membr. Sci.* 208:375–88
58. Ito Y, Ochiai Y, Park YS, Imanishi Y. 1997. pH-sensitive gating by conformational change of a polypeptide brush grafted onto a porous polymer membrane. *J. Am. Chem. Soc.* 119:1619–23
59. Ito Y, Park YS, Imanishi Y. 1997. Visualization of critical pH-controlled gating of a porous membrane grafted with polyelectrolyte brushes. *J. Am. Chem. Soc.* 119:2739–40
60. Cunliffe D, Alarcon CD, Peters V, Smith JR, Alexander C. 2003. Thermoresponsive surface-grafted poly(*N*-isopropylacrylamide) copolymers: effect of phase transitions on protein and bacterial attachment. *Langmuir* 19:2888–99
61. Nath N, Chilkoti A. 2002. Creating "smart" surfaces using stimuli responsive polymers. *Adv. Mater.* 14:1243–47
62. Rosso F, Barbarisi A, Barbarisi M, Petillo O, Margarucci S, et al. 2003. New polyelectrolyte hydrogels for biomedical applications. *Mater. Sci. Eng. C* 23:371–76
63. Ichimura K. 2003. Molecular amplification of photochemical events. *J. Photochem. Photobiol. A* 158:205–14
64. Anastasiadis SH, Retsos H, Pispas S, Hadjichristidis N, Neophytides S. 2003. Smart polymer surfaces. *Macromolecules* 36:1994–99
65. Chegel VI, Raitman OA, Lioubashevski O, Shirshov Y, Katz E, Willner I. 2002. Redox-switching of electrorefractive, electrochromic, and conductivity functions of Cu^{2+}/polyacrylic acid films associated with electrodes. *Adv. Mater.* 14:1549–53
66. Sun S, Wong YW, Yao KD, Mak AFT. 2000. A study on mechano-electro-chemical behavior of chitosan/poly(propylene glycol) composite fibers. *J. Appl. Polym. Sci.* 76:542–51
67. Tatham AS, Shewry PR. 2000. Elastomeric proteins: biological roles, structures and mechanisms. *Trends Biochem. Sci.* 25:567–71
68. Okuzaki H, Hattori T. 2003. Electrically induced anisotropic contraction of polypyrrole films. *Synth. Met.* 135:45–46
69. Hulteen JC, Jirage KB, Martin CR. 1998. Introducing chemical transport selectivity into gold nanotubule membranes. *J. Am. Chem. Soc.* 120:6603–4
70. Jirage K, Hulteen J, Martin CR. 1997. Nanotubule-based molecular-filtration membranes. *Science* 278:655–58
71. Velada JL, Liu Y, Huglin MB. 1998. Effect of pH on the swelling behaviour of hydrogels based on *N*-isopropylacrylamide with acidic comonomers. *Macromol. Chem. Phys.* 199:1127–34
72. Buehler KL, Anderson JL. 2002. Solvent effects on the permeability of membrane-supported gels. *Ind. Eng. Chem. Res.* 41:464–72
73. Beltran S, Baker JP, Hooper HH, Blanch HW, Prausnitz JM. 1991. Swelling equilibria for weakly ionizable, temperature-sensitive hydrogels. *Macromolecules* 24:549–51
74. Pelton R. 2000. Temperature-sensitive aqueous microgels. *Adv. Colloid Interface Sci.* 85:1–33
75. Afrassiabi A, Hoffmann AS, Cadwell LA. 1987. Effect of temperature on the release rate of biomolecules from thermally reversible hydrogels. *J. Membr. Sci.* 33:191–200
76. Lee WF, Huang YL. 2000. Thermoreversible hydrogels XIV. Synthesis and swelling behavior of the (*n*-isopropylacrylamide-*co*-2-hydroxyethyl methacrylate) copolymeric hydrogels. *J. Appl. Polym. Sci.* 77:1769–81
77. Hirokawa Y, Tanaka T. 1984. Volume phase-transition in a nonionic gel. *J. Chem. Phys.* 81:6379–80
78. Mendez S, Curro JG, McCoy JD, Lopez GP. 2005. Computational modeling of the temperature-induced structural changes of tethered poly(*N*-isopropylacrylamide) with self-consistent field theory. *Macromolecules* 38:174–81
79. Kim SJ, Lee CK, Lee YM, Kim SI. 2003. Preparation and characterization of thermosensitive poly(*N*-isoipropylacrylamide)/poly(ethylene oxide) semi-interpenetrating polymer networks. *J. Appl. Polym. Sci.* 90:3032–36

80. Annaka M, Sugiyama M, Kasai M, Nakahira T, Matsuura T, et al. 2002. Transport properties of comb-type grafted and normal-type *N*-isopropylacrylamide hydrogel. *Langmuir* 18:7377–83
81. Chu LY, Niitsuma T, Yamaguchi T, Nakao S. 2003. Thermoresponsive transport through porous membranes with grafted PNIPAM gates. *AlChE J.* 49:896–909
82. Arrigan DWM. 2004. Nanoelectrodes, nanoelectrode arrays and their applications. *Analyst* 129:1157–65
83. Matsumoto F, Harada M, Koura N, Nishio K, Masuda H. 2004. Fabrication and electrochemical behavior of nanodisk electrode arrays with controlled interval using ideally ordered porous alumina. *Electrochem. Solid State Lett.* 7:E51–53
84. Sun P, Mirkin MV. 2006. Kinetics of electron-transfer reactions at nanoelectrodes. *Anal. Chem.* 78:6526–34
85. Wang JY, Rongrong X, Baomin T, Renschler CL, White CA. 1994. Nanoband electrodes for electrochemical stripping measurements down to the attomole range. *Anal. Chim. Acta* 293:43–48
86. Krapf D, Wu MY, Smeets RMM, Zandbergen HW, Dekker C, Lemay SG. 2006. Fabrication and characterization of nanopore-based electrodes with radii down to 2 nm. *Nano Lett.* 6:105–9
87. Blom T, Welch K, Stromme M, Coronel E, Leifer K. 2007. Fabrication and characterization of highly reproducible, high resistance nanogaps made by focused ion beam milling. *Nanotechnology* 18:285–301
88. White RJ, White HS. 2008. Electrochemistry in nanometer-wide electrochemical cells. *Langmuir* 24:2850–55
89. Gardner CE, Unwin PR, Macpherson JV. 2005. Correlation of membrane structure and transport activity using combined scanning electrochemical-atomic force microscopy. *Electrochem. Commun.* 7:612–18
90. Aviram A, Ratner MA. 1974. Molecular rectifiers. *Chem. Phys. Lett.* 29:277–83
91. Baresel D, Gellert W, Sarholz W, Scharner P. 1984. Influence of catalytic activity on semiconducting metal-oxide sensors. 1. Experimental sensor characteristics and their qualitative interpretation. *Sens. Actuators* 6:35–50
92. Wanekaya AK, Chen W, Myung NV, Mulchandani A. 2006. Nanowire-based electrochemical biosensors. *Electroanalysis* 18:533–50
93. Fan ZY, Lu JG. 2006. Chemical sensing with ZnO nanowire field-effect transistor. *IEEE Trans. Nanotechnol.* 5:393–96
94. Swint AL, Bohn PW. 2004. Effect of acidic and basic surface dipoles on the depletion layer of indium tin oxide as measured by in-plane conductance. *Appl. Phys. Lett.* 84:61–63
95. Swint AL, Bohn PW. 2004. Effect of the interfacial chemical environment on in-plane electronic conduction of indium tin oxide: role of surface charge, dipole magnitude and carrier injection. *Langmuir* 20:4076–84
96. Zhou C, Muller CJ, Deshpande MR, Sleight JW, Reed MA. 1995. Microfabrication of a mechanically controllable break junction in silicon. *Appl. Phys. Lett.* 67:1160–62
97. Boussaad S, Tao NJ. 2002. Atom-size gaps and contacts between electrodes fabricated with a self-terminated electrochemical method. *Appl. Phys. Lett.* 80:2398
98. Rodrigues V, Fuhrer T, Ugarte D. 2000. Signature of atomic structure in the quantum conductance of gold nanowires. *Phys. Rev. Lett.* 85:4124–27
99. Bogozi A, Lam O, He H, Li C, Tao NJ, et al. 2001. Molecular adsorption onto metallic quantum wires. *J. Am. Chem. Soc.* 123:4585–90
100. Castle PJ, Bohn PW. 2005. Interfacial scattering at electrochemically fabricated atom-scale junctions between thin gold film electrodes in a microfluidic channel. *Anal. Chem.* 77:243–49
101. Dadosh T, Gordin Y, Krahne R, Khivrich I, Mahalu D, et al. 2005. Measurement of the conductance of single conjugated molecules. *Nature* 436:677–80
102. Dameron AA, Ciszek JW, Tour JM, Weiss PS. 2004. Effects of hindered internal rotation on packing and conductance of self-assembled monolayers. *J. Phys. Chem. B* 108:16761–67
103. Venkataraman L, Klare JE, Nuckolls C, Hybertsen MS, Steigerwald ML. 2006. Dependence of single-molecule junction conductance on molecular conformation. *Nature* 442:904–7
104. Chen F, Hihath J, Huang Z, Li X, Tao NJ. 2007. Measurement of single molecule conductance. *Ann. Rev. Phys. Chem.* 58:535–64
105. Chen F, Qing Q, Ren L, Wu Z, Liu Z. 2005. Electrochemical approach for fabricating nanogap electrodes with well controllable separation. *Appl. Phys. Lett.* 86:123105–7

106. Liu B, Xiang J, Tian J-H, Zhong C, Mao B-W, et al. 2005. Controllable nanogap fabrication on microchip by chronopotentiometry. *Electrochim. Acta* 50:3041–47
107. Ward DR, Grady NK, Levin CS, Halas NJ, Wu Y, et al. 2007. Electromigrated nanoscale gaps for surface-enhanced Raman spectroscopy. *Nano Lett.* 7:1396–400
108. Tao NJ. 2005. Electrochemical fabrication of metallic quantum wires. *J. Chem. Ed.* 82:720–26
109. Zach MP, Inazu K, Ng KH, Hemminger JC, Penner RM. 2002. Synthesis of molybdenum nanowires with millimeter-scale lengths using electrochemical step edge decoration. *Chem. Mater.* 14:3206–16
110. Thompson M, Menke E, Martens CC, Penner RM. 2006. Shrinking nanowires by kinetically controlled electrooxidation. *J. Phys. Chem. B* 110:36–41
111. Walter EC, Favier F, Penner RM. 2002. Palladium mesowire arrays for fast hydrogen sensors and hydrogen-actuated switches. *Anal. Chem.* 74:1546–53
112. Murray BJ, Newberg JT, Walter EC, Li Q, Hemminger J, Penner RM. 2004. Reversible resistance modulation in mesoscopic silver wires induced by exposure to amine vapor. *Anal. Chem.* 77:5205–14
113. Gu LQ, Cheley S, Bayley H. 2002. Prolonged residence time of a noncovalent adapter, β-cyclodextrin, within the lumen of mutant α-hemolysin pores. *Biophys. J.* 82:200A
114. Bayley H, Cremer PS. 2001. Stochastic sensors inspired by biology. *Nature* 413:226–30
115. Braha O, Gu LQ, Zhou L, Lu XF, Cheley S, Bayley H. 2000. Simultaneous stochastic sensing of divalent metal ions. *Nat. Biotechnol.* 18:1005–7
116. Henrickson SE, Misakian M, Robertson B, Kasianowicz JJ. 2000. Driven DNA transport into an asymmetric nanometer-scale pore. *Phys. Rev. Lett.* 85:3057–60
117. Shim JW, Gu LQ. 2007. Stochastic sensing on a modular chip containing a single-ion channel. *Anal. Chem.* 79:2207–13
118. Choi Y, Baker LA, Hillebrenner H, Martin CR. 2006. Biosensing with conically shaped nanopores and nanotubes. *Phys. Chem. Chem. Phys.* 8:4976–88
119. Harrell CC, Choi Y, Horne LP, Baker LA, Siwy ZS, Martin CR. 2006. Resistive-pulse DNA detection with a conical nanopore sensor. *Langmuir* 22:10837–43
120. Ervin EN, White RJ, Owens TG, Tang JM, White HS. 2007. AC conductance of transmembrane protein channels. The number of ionized residue mobile counterions at infinite dilution. *J. Phys. Chem. B* 111:9165–71
121. Chen M, Khalid S, Sansom MSP, Bayley H. 2008. Outer membrane protein G: engineering a quiet pore for biosensing. *Proc. Natl. Acad. Sci. USA* 105:6272–77
122. Robertson JWF, Rodrigues CG, Stanford VM, Rubinson KA, Krasilnikov OV, Kasianowicz JJ. 2007. Single-molecule mass spectrometry in solution using a solitary nanopore. *Proc. Natl. Acad. Sci. USA* 104:8207–11

Annual Review of
Analytical Chemistry

Volume 2, 2009

Contents

Errata

An online log of corrections to *Annual Review of Analytical Chemistry* articles may be found at http://anchem.annualreviews.org/errata.shtml